

neglected Fresnel reflections. Γ_0 corresponds to the initial growth of the filter produced by Fresnel reflections over the short time t_0 . This is equivalent to a transient regime which is left out of our model, our time origin is taken at $t = t_0$.

Figure 2 shows good agreement between the experiment and the calculated value of $R(t)$. Note that the fitting procedure is not a simple fit of an arbitrary function to experimental data; it is governed by the physical nature of the problem, as a direct result of the coupled-mode theory. The values obtained for α and Γ_0 are, respectively, $0.42 \text{ m}^{-1} \text{ s}^{-1}$ and $6 \times 10^{-14} \text{ m}^{-1}$. As a by-product of this numerical evaluation, the distribution of Γ along the axis of the fiber and its evolution with time are obtained as shown in Fig. 3, from which the mean value of the final relative index variation is estimated to be $\langle \Delta n \rangle / n = 10^{-7}$. Finally, given a power density $P = 1 \text{ MW/cm}^2$, and defining a photosensitivity factor

$$\beta = \frac{\partial(\Delta\epsilon/\epsilon)}{\partial t} / P = 4\alpha/kP, \quad (14)$$

we obtain $\beta = 10^{-7} (\text{MJ/cm}^2)^{-1}$ for this particular experiment.

In conclusion, the coupled-mode theory applied to this problem leads to a satisfactory model for the growth of a filter in a single-mode fiber. This theory introduces a 90° phase shift between the periodical structure and the standing-wave pattern, and it suggests that the fundamental mechanism is associated with an energy gradient rather than the energy itself. This result may give further clues as to the precise nature of the phenomenon.

This work was supported by the Federal Department of Communications under Contract OSU79-00234.

¹K. O. Hill, Y. Fujii, D. C. Johnson, and B. S. Kawasaki, *Appl. Phys. Lett.* **32**, 647 (1978).

²B. S. Kawasaki, K. O. Hill, D. C. Johnson, and Y. Fujii, *Opt. Lett.* **3**, 66 (1978).

³A. Yariv, *IEEE, J. Quantum Electron.* **QE-9**, 919 (1973).

⁴D. C. Flanders, H. Kogelnik, R. V. Schmidt, and C. V. Shank, *Appl. Phys. Lett.* **24**, 194 (1974).

⁵H. Kogelnik, *Bell Syst. Tech. J.* **48**, 2909 (1969).

⁶C. F. Quate, C. D. W. Wilkinson, and D. K. Winslow, *Proc. IEEE* **53**, 1604 (1965).

⁷H. Kogelnik, *Bell Syst. Tech. J.* **55**, 109 (1976).

Blue laser action by the rare-gas halide trimer Kr_2F

F. K. Tittel, M. Smayling, and W. L. Wilson

Rice Quantum Institute and Electrical Engineering Department, Rice University, Houston, Texas

G. Marowsky

Max-Planck-Institut für biophysikalische Chemie, Abteilung Laserphysik, D-3400 Göttingen, Federal Republic of Germany

(Received 16 June 1980; accepted for publication 4 September 1980)

Blue Kr_2F excimer laser emission centered at 430 nm has been achieved in electron-beam-pumped high-density Ar/Kr/Nf₃ mixtures. An output power of about 5 kW has been obtained. The spectral bandwidth is 25 nm for a simple two-mirror resonator with a potential tuning range between 380 and 480 nm.

PACS numbers: 42.55.Hq, 42.60.By

The recent discovery of broadband emission from several triatomic rare-gas halogen exciplex molecules¹⁻⁵ and laser action from electron-beam-pumped Xe_2Cl (Ref. 6) has led to a new class of tunable excimer lasers. Like their diatomic counterparts, triatomic excimer lasers are of considerable interest in numerous applications because of their potentially high efficiency, ready scalability to larger energies, and broad wavelength tunability in the UV and visible region of the spectrum. In this letter we report the first experimental observation of stimulated emission in Kr_2F centered at 430 nm from electron-beam-excited Ar/Kr/NF₃ mixtures. Kinetics and spectroscopy properties, in particular absorption and gain observations, of excited high-pressure Ar/Kr/F₂ and Ne/Kr/F₂ mixtures have been previously reported in the literature.^{7,8}

The experimental arrangement shown in Fig. 1 is similar to that used for the Xe_2Cl excimer laser.^{6,9} Excitation is produced by short, intense electron beam pulses (1 MeV, 15

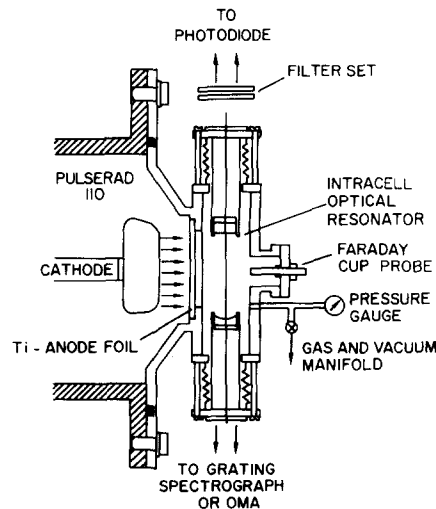


FIG. 1. Experimental arrangement for Kr_2F excimer laser.

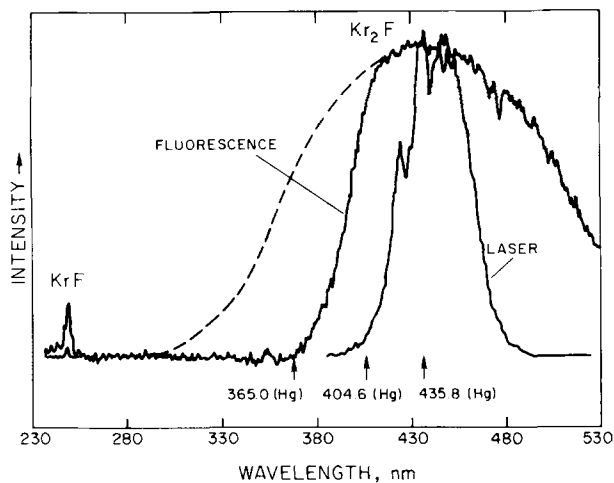


FIG. 2. Low-resolution Kr_2F fluorescence and laser spectrum for a mixture of 16-Torr NF_3 , 400-Torr Kr, and 8-atm Ar. The dashed line represents the expected fluorescence profile when taking into account the PAR 1205D vidicon spectral response below 410 nm. The OMA resolution was 0.569 nm per channel.

ka, and 10 ns) from a Physics International Pulserad 110 accelerator. The pump pulses are transversely injected through a 50- μm titanium foil over a 10- cm^2 active area into a stainless-steel reaction chamber filled with rare-gas-halogen mixtures. An intracell high- Q laser cavity was used to minimize resonator losses, which are important for a low-gain laser medium such as Kr_2F . The optical cavity was formed by two dielectric-coated mirrors: a spherical end mirror ($r = 5$ m, $R > 99.8\%$), and a flat output coupler (typically $T = 4\%$ from 410 to 440 nm) spaced 10 cm apart. Since the laser intensity depended critically on the mirror adjustment, provision was made for convenient and precise resonator alignment from outside the reaction cell. The spontaneous and stimulated emissions were characterized by a PAR OMA 1 optical multichannel analyzer and by a fast ITT F4000 S5 photodiode and Tektronix 7912 transient digitizer or 7834 storage oscilloscope.

Typical time-integrated OMA fluorescence and laser spectra for the 420-nm band are shown in Fig. 2 for a gas mixture of 16-Torr NF_3 , 400-Torr Kr, and 8-atm Ar. The fluorescence, centered at 420 nm, has a spectral bandwidth of 145 nm (FWHM), which is typical of bound-free transitions between a strongly bound ionic upper state and a repulsive covalent lower state^{2,10} of RG_2X molecules (RG is a rare gas, X a halogen). Some weak, though distinct, absorption features are apparent in the fluorescence spectrum. The Kr_2F laser spectrum exhibits characteristic spectral narrowing (to 25 nm FWHM), and red shifting with a peak centered at 430 nm. Enhanced intracavity atomic and molecular absorptions are clearly discernable, particularly in the high-resolution laser spectrum shown in Fig. 3. As in the Xe_2Cl case,⁶ the absorptions may be attributed to transient species involving the buffer gas and the active constituents (Kr, NF_3). A previously reported⁸ strong absorption peak at 358 nm was not apparent since it is outside the laser bandwidth. However, the strong absorption at 441 nm corresponds to the absorption at 441.6 nm reported in Ref. 10. Further ex-

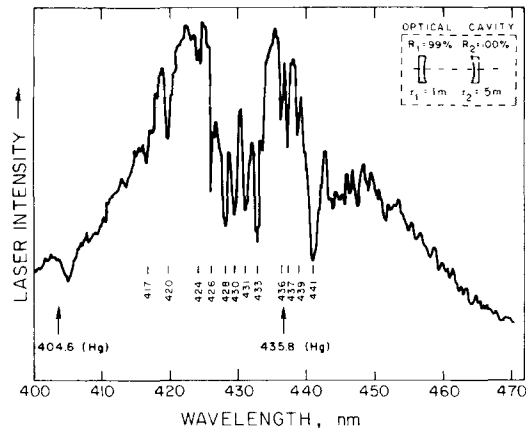


FIG. 3. High-resolution Kr_2F laser spectrum showing cavity-enhanced absorption features for a rare-gas halide mixture of 4-Torr NF_3 , 200-Torr Kr, and 8-atm Ar. The OMA resolution was 0.143 nm per channel.

periments will establish whether different gas mixtures or lower temperatures will affect these visible absorption effects^{5,8} and enhance Kr_2F stimulated emission.

The spectrally resolved temporal behavior of the laser emission is shown in Fig. 4. Also shown is a reference electron beam pulse, as monitored by a Faraday probe. The electron beam peak current density was 110 A/cm^2 at the optical axis some 1.5 cm from the anode foil. The pulse width of the spontaneous emission was typically 110 nsec. The pulse width for stimulated emission was as short as ~ 30 nsec, with the pulse duration being strongly dependent upon the cavity Q . The fluorescence and laser signals peaked 20 and 40 nsec, respectively, after the peak of the electron beam pulse of 10-nsec duration. The delayed appearance of the laser output is consistent with that observed for Xe_2Cl ,^{6,11} caused by the initial strong transient absorptions induced by the electron beam pulse. Both transient absorption effects and the interaction of the cavity radiation field with the excited species could modify the kinetic channels, leading to the formation of Kr_2F^* . Some evidence of this modification is suggested by the quenching of the main $\text{KrF}(B \rightarrow X)$ line at 248 nm when the laser cavity is aligned. The output power of the Kr_2F laser, as estimated from the sensitivity of the photodiode, was ~ 5 kW at 8 atm of argon buffer gas. The measured beam divergence was 3 mrad.

The stimulated-emission cross section can be estimated based on the fluorescence spectrum and decay time. The excimer-gain cross section is given by^{10,11}

$$\sigma = (1/8\pi c \Gamma) (\lambda^4 / \Delta \lambda),$$

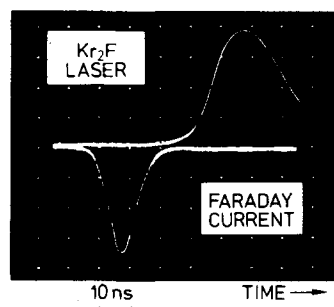


FIG. 4. Typical data set showing temporal behavior of laser and electron beam pulses. A mixture 16-Torr NF_3 , 400-Torr Kr, and 8-atm Ar was used with a high Q resonator ($r = 5$ m, $R > 99.8\%$ and $r = \infty$, $R = 96\%$). The peak current is 110 A/cm^2 at 1.5 cm from the anode foil in pure argon at 3 atm.

where Γ is the spontaneous decay time and $\Delta\lambda$ is the FWHM of the fluorescence spectrum. For Kr_2F : $\lambda \sim 420$ nm, $\Delta\lambda \sim 145$ nm, and $\Gamma \sim 110$ nsec. This gives a $\sigma_{\text{Kr}_2\text{F}} \sim 2.5 \times 10^{-18}$ cm², which is considerably less than $\sigma_{\text{KrF}} = 2 \times 10^{-16}$ cm² for the main line KrF transition. The gain coefficient g_0 may be expressed by $g_0 = \sigma N^*$, where the value of the upper-laser-state density may be determined by comparing it to a previously analyzed laser system, such as $\text{XeF}(C \rightarrow A)$ or $\text{N}_2(C \rightarrow B)$. For $N^* = 10^{16}$ cm⁻³, $g_{\text{calc}} \approx 0.02$ cm⁻¹ which is in agreement with g_{thresh} obtained by establishing the laser threshold reflectivity of the cavity output coupler ($\sim 96\%$).

In summary, a new triatomic exciplex laser has been operated in the deep blue band of Kr_2F , which extends the tuning range of excimer lasers from the green to the blue-UV spectral region. The laser output has a bandwidth of 25 nm centered at 430 nm, and a peak power of several kW was observed. The stimulated emission cross section was estimated to be about 2.5×10^{-18} cm² in the afterglow of electron-beam-excited mixtures of Ar/Kr/Nf₃. The wavelength tunability of this triatomic excimer laser was established by an observed peak-wavelength shift of 10 nm for two sets of cavity reflectors, one centered at 425 nm and the other at 400 nm. To obtain broadband continuous tunability over a potential tuning range of 100 nm, as estimated from the fluores-

cence spectrum, it will be necessary to employ a low-loss wavelength-selective cavity. This can be accomplished, for example, by placing the cavity end mirror by a dispersive Littrow prism reflector.

This work was supported by the Office of Naval Research, the National Science Foundation, and the Robert A. Welch Foundation.

¹D. C. Lorents, D. L. Huestis, M. V. McCusker, H. H. Nakano, and R. M. Hill, *J. Chem. Phys.* **68**, 4657 (1978).

²D. L. Huestis and N. E. Schlotter, *J. Chem. Phys.* **69**, 3100 (1978).

³J. A. Mangano, J. H. Jacob, M. Rokin, and A. Hawryluk, *Appl. Phys. Lett.* **31**, 26 (1977).

⁴W. R. Wadt and P. J. Hay, *J. Chem. Phys.* **68**, 3850 (1978).

⁵N. G. Basov, V. A. Nanliychev, V. A. Dolgikh, O. M. Kerimov, V. S. Lebedev, and A. G. Molchanov, *JETP Lett.* **26**, 16 (1977); also V. S. Zuev (private communication).

⁶F. K. Tittel, W. L. Wilson, R. E. Stickel, G. Marowsky, and W. E. Ernst, *Appl. Phys. Lett.* **36**, 405 (1980).

⁷R. O. Hunter, J. Oldenettel, C. Howton, and M. V. McCusker, *J. Appl. Phys.* **49**, 549 (1978).

⁸J. G. Eden, R. S. F. Chang, and L. J. Palumbo, *IEEE J. Quantum Electron.* **QE-15**, 1148 (1979).

⁹G. Marowsky, R. Cordray, F. K. Tittel, and W. L. Wilson, *Appl. Opt.* **17**, 3491 (1978).

¹⁰*Excimer Lasers*, edited by Ch. K. Rhodes (Springer, Berlin, 1979).

¹¹K. Y. Tang, D. C. Lorents, and D. L. Huestis, *Appl. Phys. Lett.* **36**, 347 (1980).

Nonlinear optical properties of *N, N'* dimethylurea ^{a)}

J.M. Halbout, A. Sarhangi, and C.L. Tang

Optical Phenomena Study Group, Materials Science Center, Cornell University, Ithaca, New York 14853

(Received 6 August 1980; accepted for publication 4 September 1980)

The performance of a nonlinear organic material, *N, N'* dimethylurea, is evaluated through second-harmonic generation in powder. It is shown to be most effective in the region 227–240 nm. The UV absorption of this compound is also reported. The observation of second harmonic generation in this material rules out one of the two crystal structures reported in the literature.

PACS numbers: 42.65.Cq

Nonlinear crystals are extensively used for generating UV radiation from powerful visible sources. The spectral region from 200 to 250 nm can be reached conveniently only through second-harmonic generation (SHG) in KB5, for which the phase matching cutoff occurs at 217 nm,¹ or through sum frequency mixing (SFM) in some of the KDP isomorphs (218 nm in KDP²) or in KB5 (187 nm).³ It has recently been shown that urea, an organic crystal, can be advantageously used down to 240 nm in SHG or 229 nm in SFM.⁴ In this letter we report measurements on powder samples of *N, N'* dimethylurea which show that this material can generate 227-nm radiation through straight second-harmonic generation and is considerably more efficient than KB5.

N, N' dimethylurea is reported to crystallize in the orthorhombic systems.^{5,6} However, two different crystal classes can be found in the literature for this material: *mmm* (D_{2h}^{13}),⁵ and *mm2* (C_{2v}).⁶ The observation of second-harmonic generation in powder samples of *N, N'* dimethylurea rules out the former of these classes for it has a center of inversion.

Details of the experimental setup will be given elsewhere.⁷ In brief, samples of 1-mm thickness, consisting of 100–150- μm grains immersed in index matching fluid, were illuminated by a Nd:YAG laser-pumped dye laser (300–500 kW peak power and 2 mm beam diameter). *N, N'* dimethylurea was previously purified by successive recrystallization from acetone. The second harmonic was detected either by a photodiode or by a solar-blind photomultiplier after removal of the fundamental through color filters or a quarter-meter monochromator, and averaged on a boxcar integrator. The

^{a)}Work supported by the National Science Foundation.